4

Spinor BEC apparatus

In this chapter I describe the apparatus used to create and study spinor condensates. Magneto-optical trapping and evaporation down to BEC is a standard procedure, covered in detail elsewhere [51, 136]. I therefore present only a brief overview of the experimental apparatus, followed by details on the unique contributions I have made to this apparatus. The interested reader is referred to the thesis of A. A. Wood [137] for further information on the design of the apparatus, choice of components, and the experiment staging required to produce a BEC.

4.1: The Bose-Einstein condensate factory

The layout of the condensate apparatus (Figure 4.1) follows the general design of Lin *et al.* [138], modified to include a large glass cell 'science chamber'. Atoms are sourced from a $5\,\mathrm{g}$ rubidium-87 ampule loaded into an oven, which is heated to $80^{\circ}\mathrm{C}$ and monitored by an interlock (see §4.3). This creates an effusive atom beam through a collimation tube towards a cold-cup [139], which both performs cyro-pumping and further collimation by capturing any atoms not travelling down the desired axis of the beam.[1]

The atoms then enter a zero-crossing single-layer tapered Zeeman slower [140, 141], which creates a spatially varying magnetic field that counters the Doppler shift and enables a counter-propagating laser beam to slow atoms from $380\,\mathrm{m/s}$ to $20\,\mathrm{m/s}$ [142]. The atoms are then loaded into a six-beam Magneto-Optical Trap (MOT) based on variable-magnification beam-expanders [143] that create large-diameter MOT beams and increase the number of atoms caught in the trap. The MOT has a total power of $\approx 50\,\mathrm{mW}$ divided across its six beams, each with an approximately top-hat profile with $16\,\mathrm{mm}$ diameter. Typically the MOT captures $\sim 10^9$ atoms in a diameter of $\sim 10\,\mathrm{mm}$.

Following the MOT formation, the quadrupole field is deactivated and the atoms are polarisation-gradient cooled during an optical molasses cycle for $8\,\mathrm{ms}$, reducing the cloud temperature to $31 \pm 3\,\mu\mathrm{K}$. The quadrupole gradient is then ramped up to $40\,\mathrm{G/cm}$ to catch the free-falling cloud in a magnetic trap, which is hybrid-loaded

[1] A pneumatic shutter blocks the atom beam unless the MOT is being loaded.

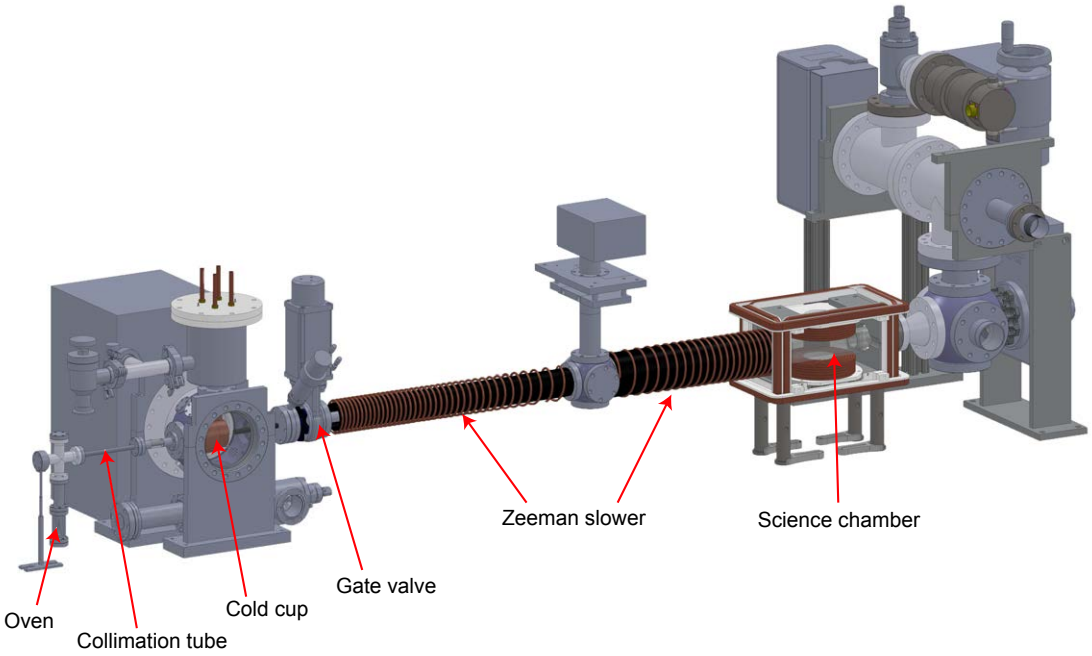

Figure 4.1: *A CAD visualisation of the vacuum system showing the trajectory of the atoms from the oven (left) into the UHV section containing the science chamber (right). Optics and MOT assembly not shown.*

into a crossed-beam optical dipole trap formed by a KEOPSYS 1064 nm 20 W single-mode, linearly polarised fiber laser. Finally, forced evaporation is carried out in the crossed-beam dipole trap to achieve condensation. Typically this produces a BEC with $\sim 3 \times 10^5$ atoms and trapping frequencies of $(\omega_x, \omega_y, \omega_z) = 2\pi \times (35, 60, 80)$ Hz.

Laser cooling and imaging requires beams at several different detunings (Figure 4.2). The 'master' laser is an EAGLEYARD RWE-0810 external-cavity diode laser (ECDL) in the Littrow configuration [144, 145] that generates seed light on the $|F = 2\rangle \rightarrow |F' = 3\rangle$ pump transition, which is locked using modulation transfer spectroscopy (MTS) [146, 147] for an extremely robust laser lock. The master laser seeds an M2K UC012 master oscillator power amplifier (MOPA) chip to produce ~ 1 W of 780 nm light [148], which is divided into several arms containing Acousto-Optic Modulators (AOMs) to frequency-shift each beam to the required detuning (Figure 4.3). Two repump lasers locked to the $|F = 1\rangle \rightarrow |F' = 2\rangle$ transition are used to optically pump atoms out of the $|F = 1\rangle$ dark state. The Zeeman repump is locked using a digital offset-lock (§4.2) and the MOT repump is locked with saturated absorption spectroscopy [149].

Polarisation-maintaining fibers are used to transfer the light between different sections of the apparatus. This effectively decouples the different sections of the apparatus, preventing perturbations and accidents from misaligning the entire system. The single-mode fibers also have the addition benefit of cleaning up the poor spatial mode of the MOPA [150] by transmitting only the TEM_{00} component at the expense of losing

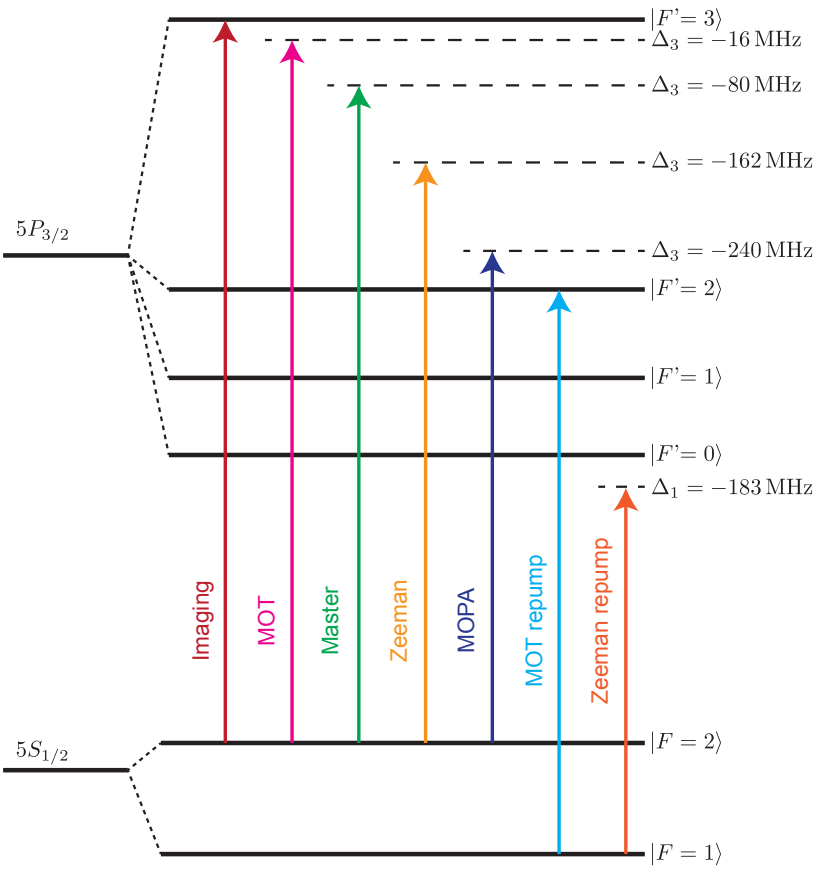

Figure 4.2: *Laser detunings used to perform cooling and trapping of ^{87}Rb atoms, measured in hertz. The master laser seeds the laser amplifier (MOPA) from which the imaging, MOT and Zeeman are derived using AOMs. The repump beams are produced by independent lasers.*

the power contained in the higher-order spatial mode components.

Magnetic field control is provided by a set of three orthogonal rectangle-based bias coil pairs, and a pair of quadrupole coils. The bias coils comprise 16 turns each in approximately Helmholtz configuration (Figure 4.4) and are operated by an in-house designed IGBT-based voltage-controlled current source called the 'Mag-neat-o'. Each coil can be driven by up to 20 A, and steady-state bias fields of 10 G can be generated without requiring active cooling.

The quadrupole coils are wound from 42 turns of square-sectioned copper tubes with side length 4.76 mm and are internally water-cooled by a closed loop chiller.[2] Each coil is multi-layered, with inner/outer diameters of 60/126 mm and are separated by approximately 90 mm in anti-Helmholtz configuration. The coil pair is capable of generating up to 300 G/cm, though the MOT is typically formed in a gradient of 14.8 G/cm.

[2] A micropump is required to achieve the desired flow rate through both the quadrupole and Zeeman slower coils; flow-rate sensors ensure the apparatus is not operated without active cooling.

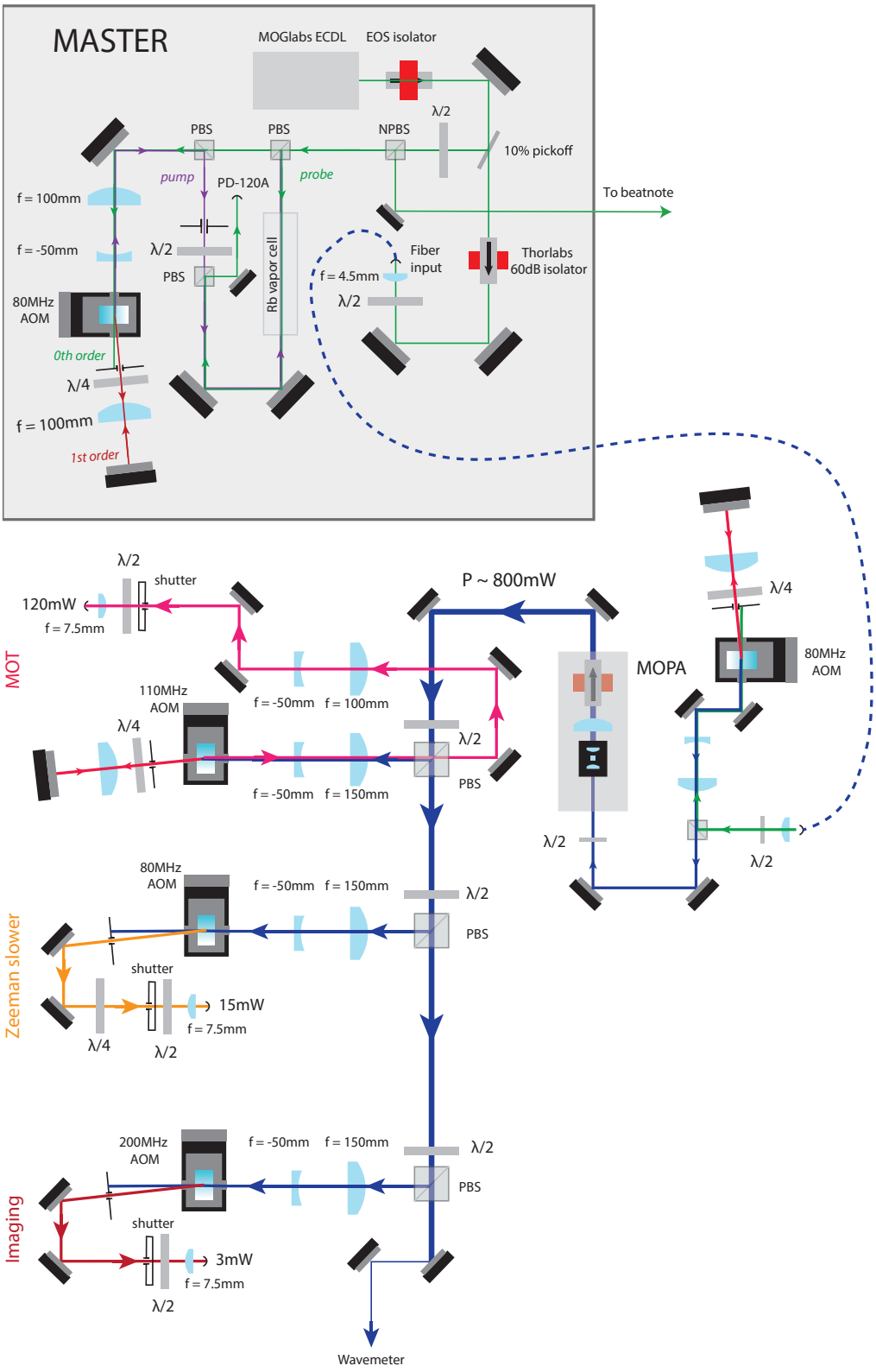

Figure 4.3: *Scheme to generate the MOT, Zeeman slower and imaging beams using a single tapered amplifier. The master laser is locked using digital MTS and fiber-coupled to the MOPA. The MOPA output is divided into several arms, which use AOMs to frequency-shift the beams to obtain the required detunings. Adapted with permission from [137].*

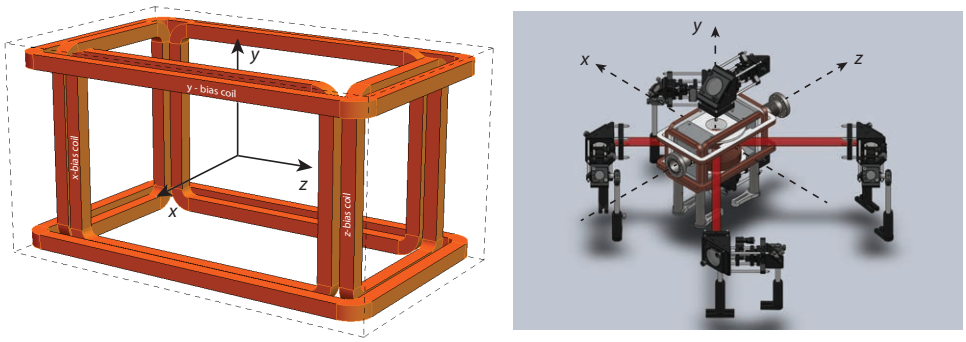

Figure 4.4: *Design of the rectangular-base magnetic field bias coils (left), and arrangement of coils around the science chamber including MOT components (right). See §8.1 for an explanation of the coordinate system. Reproduced with permission from [137].*

Radio frequency pulses are generated by direct digital synthesis (DDS) with either a RFBLASTER[3] or PULSEBLASTER DDS-II-300-AWG, and coupled to the atoms using a MINICIRCUITS LZY-22 amplifier connected to one of two radio antennae. The work presented in this thesis uses the 'side' antenna, which is a single-layer coil oriented in the y–z axis, comprised of 20 turns and having diameter 60 mm.

Microwaves are generated by a PHASEMATRIX FSW-0010 DDS, which operates at up to 10 GHz, and amplified by a MINICIRCUITS ZVE-3W-83X+ +35 dB rf-amplifier. The microwaves are coupled to the atoms with a custom half-wave dipole antenna designed for 6.834 GHz, located approximately 50 mm from the centre of the cell. Two series SKYWORKS SKY13298-360 switches allow the microwaves to be gated by a TTL trigger to prevent unintentional coupling between the hyperfine levels.

4.2: Beatnote microwave offset lock

Rubidium-87 has two hyperfine ground state energy levels, $|F = 1\rangle$ and $|F = 2\rangle$, with an energy level splitting between them of 6.834 GHz (Figure 4.5A). Typically only the $|F = 2\rangle$ state is used for cooling and trapping, but atoms promoted to an excited state can decay into either of the hyperfine ground states. Over time, atoms pumped by a cooling laser will randomly decay into the $|F = 1\rangle$ state, which is too far detuned to continue to interact with the pump laser, making it a 'dark' state.

A 'repump' laser is therefore required to perform the reverse process and optically pump atoms back into the $|F = 2\rangle$ state. However, since hyperfine splitting is large (6.8 GHz), the repump transition is not easily derived from the MOPA by modulation techniques. Furthermore, the absorption signal from the repump transition is typically very weak (Figure 4.5B) so it is difficult to reliably frequency-lock a laser there

[3] The RfBlaster is a 2-channel DDS developed in-house, based on dual AD9910S controlled by a XILINX FPGA running PETALINUX and programmed in PYTHON using a custom compiler.

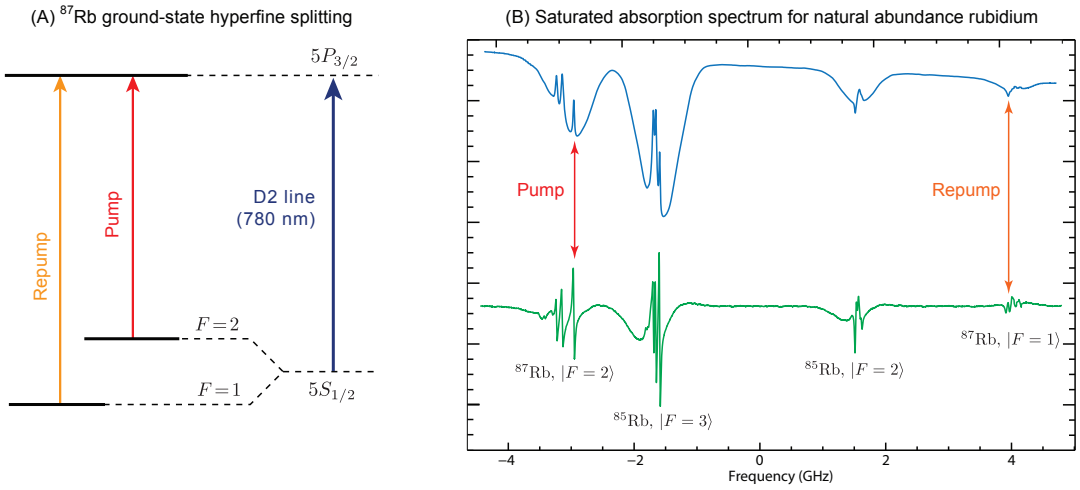

Figure 4.5: *The ground-state hyperfine splitting of ^{87}Rb (A), and the D_2 line of a natural abundance rubidium (B) showing the saturation absorption profile (blue) and derived error signal (green). Note the amplitudes of the error signal for the repump transition are significantly smaller than the pump transition.*

using standard techniques like saturated-absorption spectroscopy [149]. Alternate techniques such as modulation transfer spectroscopy [147] have been demonstrated to provide a robust method of locking the pump laser [151], but are not as successful on the repump transition because of the lack of a cycling transition.

An alternate method to locking the pump and repump lasers independently is to lock the pump to the cooling transition using an atomic reference, and then lock the repump to the pump using a beatnote. The frequency separation between the pump and repump should match the known hyperfine splitting of the isotope, so a large single-featured error-signal can be derived by comparing the frequency of the beatnote to the desired separation [152].

As the beatnote frequency (6.8 GHz) is in the microwave regime, it is necessary to use a phase-locked loop (PLL) synthesiser to divide the beatnote frequency down to the rf-domain for signal processing. The divided signal can then be compared against a stable reference at known frequency (such as GPS clock), producing an error signal for reliable laser locking (Figure 4.6).

In this scheme, a small fraction of the each of the two lasers is extracted with a PBS cube, which are then combined on an NPBS to generate a beatnote on a HAMAMATSU G4176 fast photodetector, which has a 30 ps rise time at 7 V bias [153]. The photodetector is powered via a MINICIRCUITS ZX85-12G-S+ bias-tee with 9 V DC input, and the beatnote signal is amplified by five MINICIRCUITS ZX60-8008E-S+ +8 dB amplifiers to boost the rf power to $\sim$0 dBm when 4 mW is incident on the photodetector. The resulting beatnote is processed by the PLL and compared to a stable reference frequency by a phase-frequency detector (PFD), which produces an error signal that quantifies

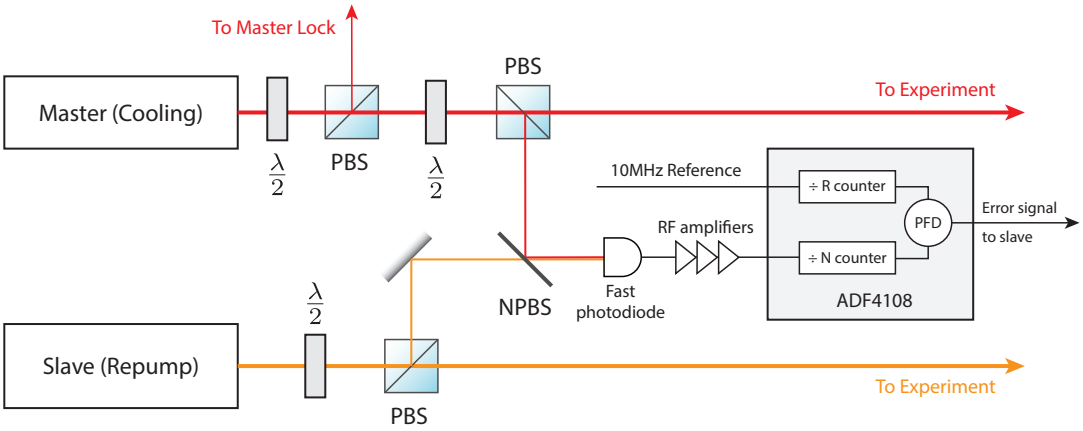

Figure 4.6: *Schematic of the digital offset-lock. A fraction of the pump and repump lasers are separated with polarising beamsplitter (PBS) cubes to form a beatnote on the non-polarising beamsplitter (NPBS) as detected on the fast photodiode.*

the difference between the measured (f_{in}) and desired (f_0) beatnote frequencies. The integrated circuit chosen for this task was the ANALOG DEVICES ADF4108 [154], for its high rf bandwidth (8 GHz) and availability in a premade evaluation-board (ANALOG EVAL-ADF4108EBZ1) to provide an interface to the chip.

The operational principle of the PLL device is to take the input f_{in} and reference f_{ref} signals and use counters to frequency-divide them by N and R respectively, where N and R are chosen such that $f_0 = N f_{\text{ref}}/R$. The resulting divided signals are compared, and if the frequencies are different then the PFD output is set to either 0 V or 5 V depending on which frequency is higher. However, if the divided frequencies are the same, the PFD outputs a voltage between 0 V and 5 V that is proportional to their difference in phase. Comparing the divided frequencies in this way is equivalent to comparing the input signal f_{in} to the target frequency f_0 and outputting a voltage proportional to their frequency difference that rails when the difference is more than the 'channel spacing' $f_{\text{pfd}} = f_{\text{ref}}/R$.

Because the beatnote frequency is so high, the N counter itself comprises a pre-scaler P and two programmable counters A and B that have the net effect of dividing the input by $N = BP + A$. There is a lot of freedom in selecting the counter values, but empirically it is best to choose the counters to limit phase noise, which is multiplied by the PFD at a rate of $20 \log N$ [155]. This implies that the counter values should be chosen to be as small as possible, subject to the operational requirements of the ADF4108 [154],

$$A < 64, \quad 2 < B < 8192, \quad f_{\text{in}}/P < 300\,\text{MHz} \quad \text{and} \quad N > P(P-1).$$

A simple algorithm that chooses the smallest values for the counter parameters for a

given desired frequency f_0 and reference frequency f_{ref} is

$$P \geq \left\lceil \frac{f_0}{300\,\text{MHz}} \right\rceil, \quad R = \left\lceil \frac{f_{\text{ref}}}{f_0} P(P-1) \right\rceil, \quad N = \left\lfloor \frac{R f_0}{f_{\text{ref}}} \right\rfloor, \quad B = \left\lfloor \frac{N}{P} \right\rfloor, \quad A = N - BP,$$

where P is the smallest power of 2 that obeys the above inequality, and values are computed in order from left to right.

The possible values for the desired frequency f_0 are discretised into multiples of the channel spacing $f_{\text{pfd}} = f_{\text{ref}}/R$. In choosing R to be small to limit noise, the channel spacing is increased and the possible values of f_0 become more coarsely spaced. However, for the repump transition it is not critical to be exactly on resonance, and being detuned by a few MHz from the optimal frequency is acceptable. In particular, the offset lock was applied to the Zeeman repump laser which is off-resonant with the zero-velocity repump transition of the MOT, instead countering the Doppler shift for atoms exiting the oven. The beatnote frequency (Table 4.1) was optimised empirically by observing MOT load rates for a range of possible detunings. It should be noted that the offset lock has the unique advantage of being able to adjust the counter settings to arbitrarily set the lock point, and is not subject to the low efficiency and limited frequency range of modulation techniques (e.g. AOMs), or properties of the atomic transition (e.g. DAVLL [156]).

Parameter	f_0	P	R	A	B	N	f_{pfd}
Value	6305 MHz	32	2	13	39	1261	5 MHz

Table 4.1: *Register settings required to lock the Zeeman repump laser using phase-frequency detection against a stable* 10 *MHz reference signal.*

The PLL-synthesiser is controlled by settings stored in three 24-bit registers, which define the operation of the internal counters and the functionality of the PFD and are programmed using 3-wire SPI through a DB-9 connector Although programmable by computer via the parallel port using the manufacturer's software, it is desirable for the lock to operate independently of workstation computers. For this purpose, the ETHERNUT V2.1B micro-controller was chosen to form a bridge between the chip and user, constructing the register settings and programming the chip via a human-friendly interface over the local Ethernet. This required writing a custom TCP-server in the Ethernut's `NutOS` operating system, calculating the required latch settings and 'bit-bashing' output over the board's general-purpose I/O.

The range of the signal output by the PLL is 0–5 V, which is beyond the input specifications of the laser controller. To interface the error signal from the PFD with the laser controller, a signal processing circuit was constructed (Figure 4.7). The 0–5 V PFD output from the charge-pump (CP) pin is fed through a gain-2 'offset' amplifier that level-shifts the input to be symmetric about zero. The subsequent variable-gain

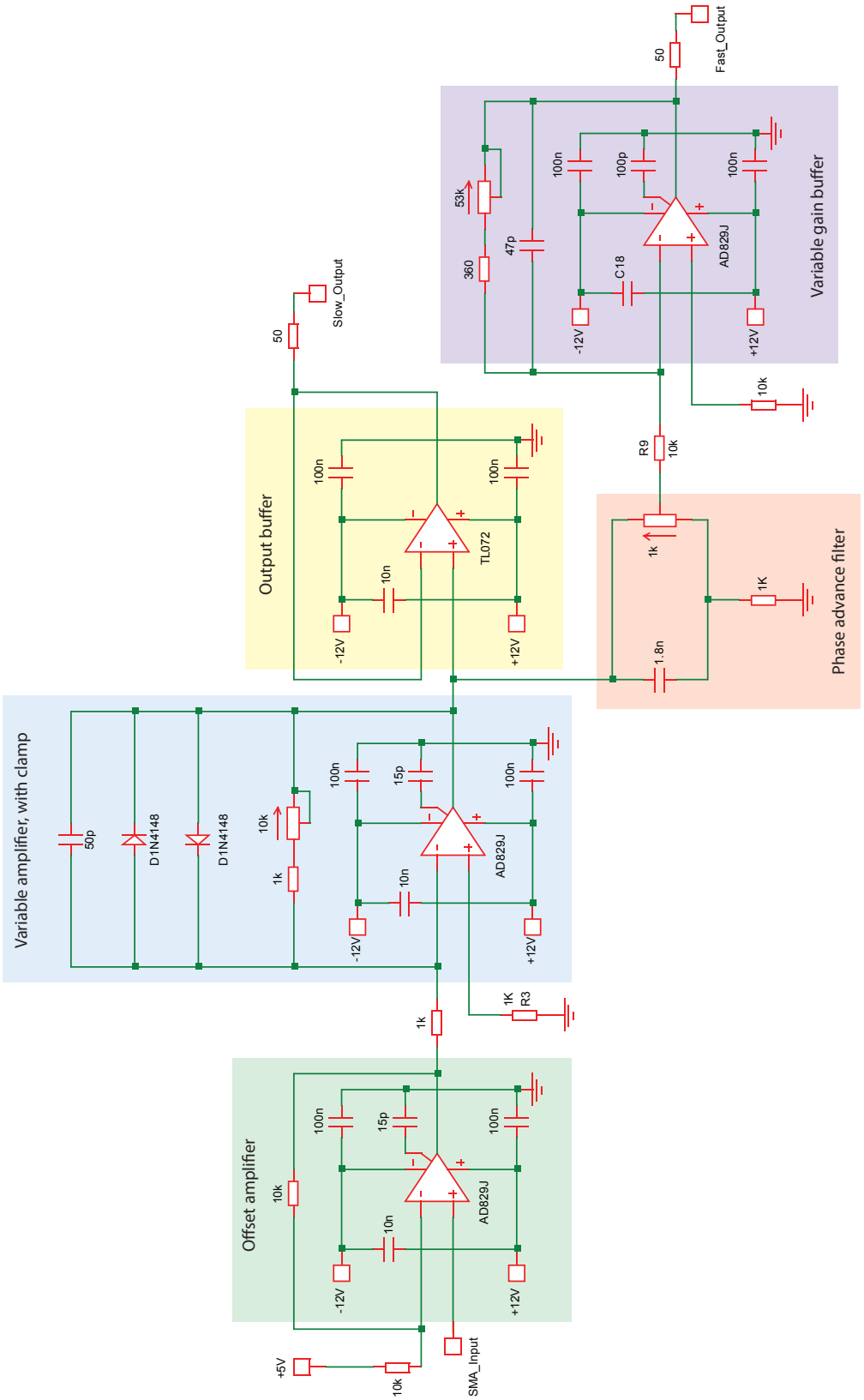

Figure 4.7: *The signal processing circuit that level-shifts, amplifies and clamps the output from the PFD to produce a 'slow' feedback signal for the laser controller and a 'fast' feedback signal for direct injection into the laser head.*

amplifier includes a protective clamp in the feedback arm to limit the range of the amplified error signal and prevent the laser entering oscillation. Two output signals are generated, one for feedback directly into the laser controller for PID locking ('slow' feedback), and the other for modulation of the laser diode current itself ('fast' feedback), for reasons which will be discussed presently.

The output of the phase-frequency detector rails when the frequencies being compared are different by more than the 'channel spacing' of the divider, typically 5 MHz. This is a tiny fraction of the beat frequency (6.8 GHz), or the frequency range of a laser scan (∼500 MHz), so for a scanning laser the output changes rapidly when the laser passes the lock point, producing a square-wave error signal. Using this error signal directly therefore produces 'bang-bang' oscillations, whereby the extremely high gain of the error-signal causes the controller to continually overshoot the locking-point.

This is caused by insufficient servo bandwidth in our laser controller, making it necessary to construct a signal-processing board to produce a 'fast'-feedback signal for direct injection into the laser headboard to bypass the slow servo loop of the controller and obtain a lock. To prevent damage to the diode, the control signal was not added directly to the diode current; rather a FET-modulation technique [152] was used to drain a small amount of current away from the diode, in proportion to a control voltage derived from the PFD (Figure 4.8). As the laser scans, its frequency ramps up and the beat frequency increases. When the beatnote hits the desired value, the PFD output jumps, changing the FET base voltage and bleeding current away from the diode and reducing the laser frequency again. This has the effect of bringing the laser frequency closer to the desired detuning, linearising the step function across a scan sweep (Figure 4.9). Hence the overall gain of the frequency comparator is reduced, enabling the 'slow' locking servo to converge on the zero point.

Correctly choosing the degree of fast feedback is very important in this circuit; too much gain produces overshoot and causes the laser frequency to oscillate rapidly, as can be observed by monitoring the beatnote on an rf spectrum analyser. Optimal locking (with minimal linewidth) is obtained when the injection gain is maintained just above the point at which the fast-feedback enables the slow laser controller to lock (Figure 4.10).

4.3: Industrial reliability with microcontroller interlocks

The design philosophy of the apparatus was that it should be able to operate in the absence of human intervention for several hours at a time; ideally capable of performing experiments overnight without supervision. An important part of such independent operation is a system of interlocks that monitor the state of the apparatus, and *automatically* take action in the event of a systems failure to render the apparatus safe.

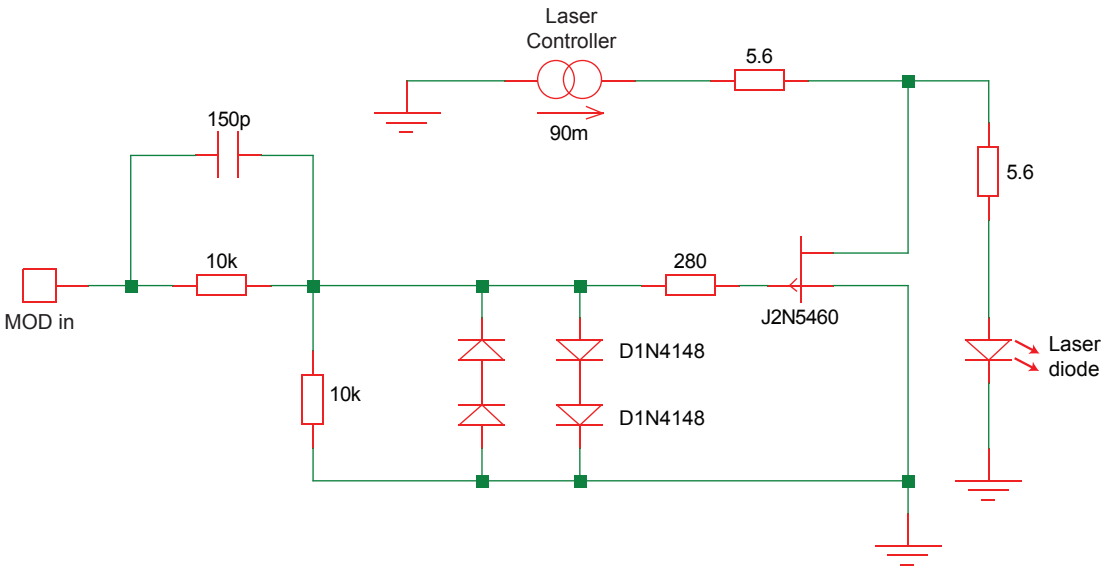

Figure 4.8: *The FET-modulation circuit to enable fast-feedback by using a control voltage to reduce the laser current, adapted from [152]. Applying a positive voltage to 'MOD in' causes the JFET to bleed a small amount of current away from the diode laser, which modulates the lasing frequency and closes the offset-lock servo loop. This is termed 'fast' feedback as it bypasses the laser controller and has a high modulation bandwidth. Since the feedback only reduces the current through the diode, there is no danger of accidentally damaging the laser by overloading it.*

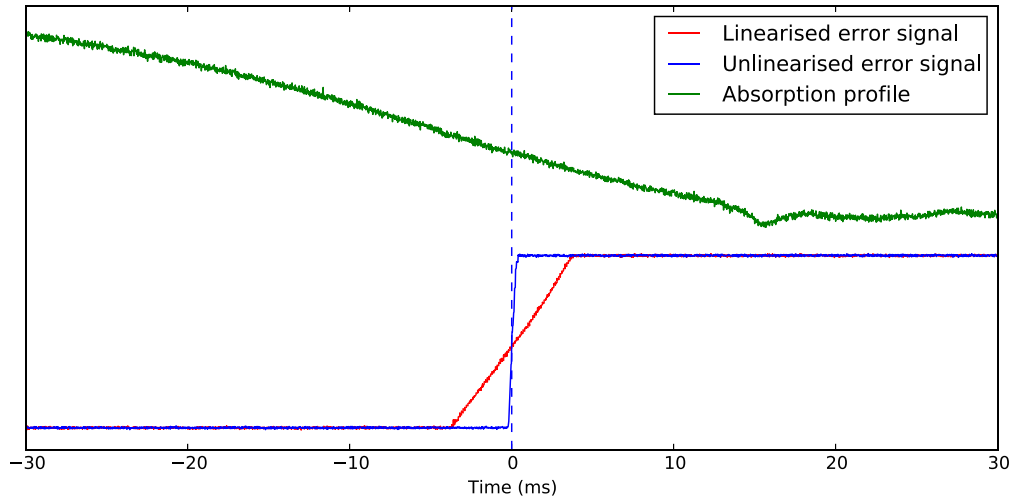

Figure 4.9: *The PLL-synthesiser compares the beatnote frequency to a desired value, producing a sharp step response as the laser scans past. Engaging the fast-feedback circuit has the effect of linearising the error signal as the frequency is scanned, reducing the overall gain of the feedback loop and producing a slope that the laser controller can lock to. A saturated absorption spectrum is provided for reference.*

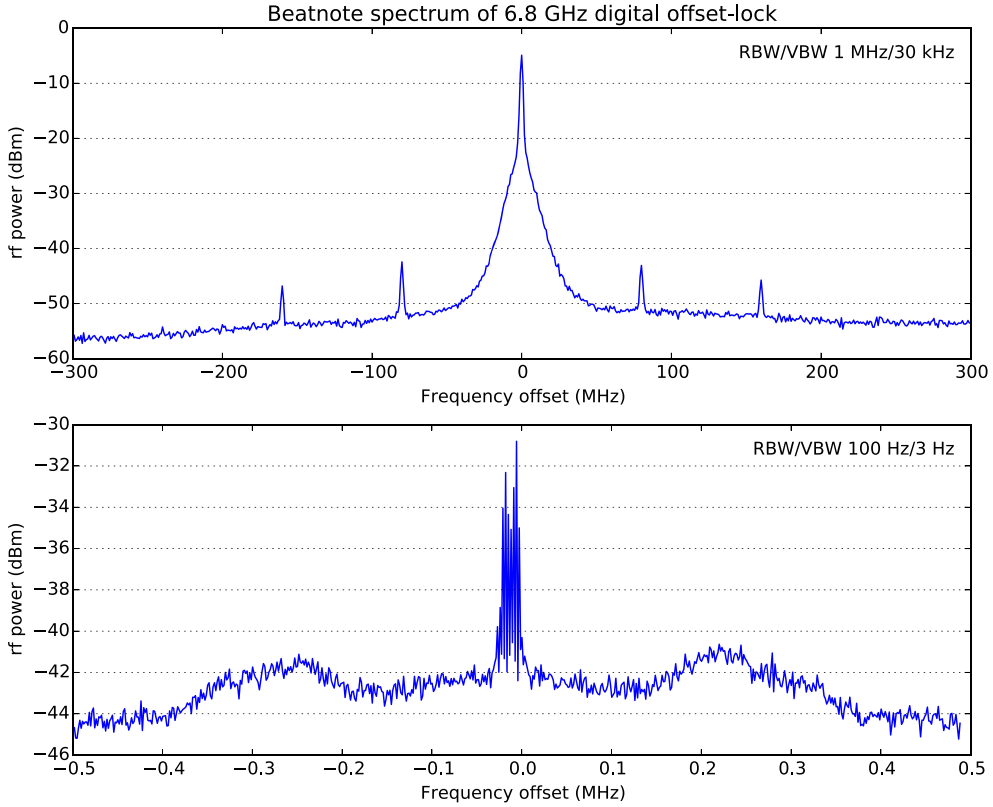

Figure 4.10: *Rf beatnote spectrum of laser locked using digital offset-lock at 6.8 GHz. The width of the central feature is less than 20 kHz, and the 'servo bump' indicates a bandwidth of at least 100 kHz.*

Rubidium is a highly reactive alkali metal, and as such the side of the vacuum system containing the rubidium ampule is separated from the science chamber by a pneumatic gate valve, which can be sealed in an emergency. An independent controller operating as a watchdog is capable of determining when an emergency occurs and closing the gate valve to seal the source to protect the rest of the chamber. Similarly, the temperature of the oven controls the atom flux, so it is desirable to have a high level of control over its operation; not just to control the temperature of the ampoule but also to ensure the oven is returned to an inert state in the event that something goes wrong.

In particular, failure of either Peltier heat exchanger or the water cooling system would prevent the cold-cup collecting atoms, and instead cause previously trapped atoms to be released. Such a failure would prevent heat being removed from the hot side of the Peltier, leading to runaway heating of the Peltier and hence the cold-cup. This would generate a rubidium 'fountain': polluting the vacuum system, damaging sensitive vacuum equipment (such as the ion pumps) and necessitating an expensive and time-consuming rebuild of the vacuum system. Of the two other research groups around the world using this design, both have reported experiencing this problem to

some degree because of a cooling system failure.

To automate control and monitoring of the oven-system, a custom control system based on the industrial GALIL RIO-47100 programmable-logic controller (PLC) was devised. The RIO controller was chosen for its large number of IO-ports, automatic and independent PID loops, and Ethernet connectivity. A finite state-machine (Figure 4.11) was written in the custom Galil 'DMC' language used by the RIO devices, to ensure that the oven controller remained in a well-defined state at all times, ensuring no dangerous actions were unintentionally initiated. The built-in PID loops were applied to control the oven heaters, enabling fast warm-up cycles and reliable temperature control to produce a consistent output flux from the oven. Details on the implementation are presented in Appendix A.

Various failure modes were considered, ranging from minor (e.g. non-critical sensor disconnection) to extreme (e.g. vacuum failure, coolant failure, runaway PID loops). Upon detection of an error, the machine enters a 'fail-safe' mode, in which all potentially dangerous devices are deactivated by isolating the chamber (sealing the gate-valve), stopping the oven (heaters and Peltiers) and alerting the user (siren, network and SMS alerts). Physical user intervention is required to restart the machine after a failure, ensuring the machine never leaves a safe 'shutdown' state on its own without human intervention to ensure it is safe. Relays on the power supplies to the oven heaters mean that even in the event of sudden power-failure to the controller, the oven is rendered safe.

For monitoring purposes, the controller communicates with a logging server that emits SYSLOG-compatible messages. Log messages are sent whenever the machine changes state, as well as periodically to provide updates on the temperature of the oven and a number of attached gauges. These messages can then be processed by a number of standard SYSLOG tools for remote viewing, monitoring and graphing, as well as post-hoc diagnosis of emergency events. The latter has been essential for identifying unforeseen failure modes, which were then accounted for in the state machine.

A number of other interlock devices were also constructed; one to turn off the 120 A Zeeman slower power supplies in the event of water cooling failure, and another to prevent damage to the MOPA by being run at too high a current, or running without a seed beam. Either of these two disaster scenarios would cause significant damage to the apparatus and is enough to significantly set-back the project; they therefore warrant their own fail-safe watchdogs.

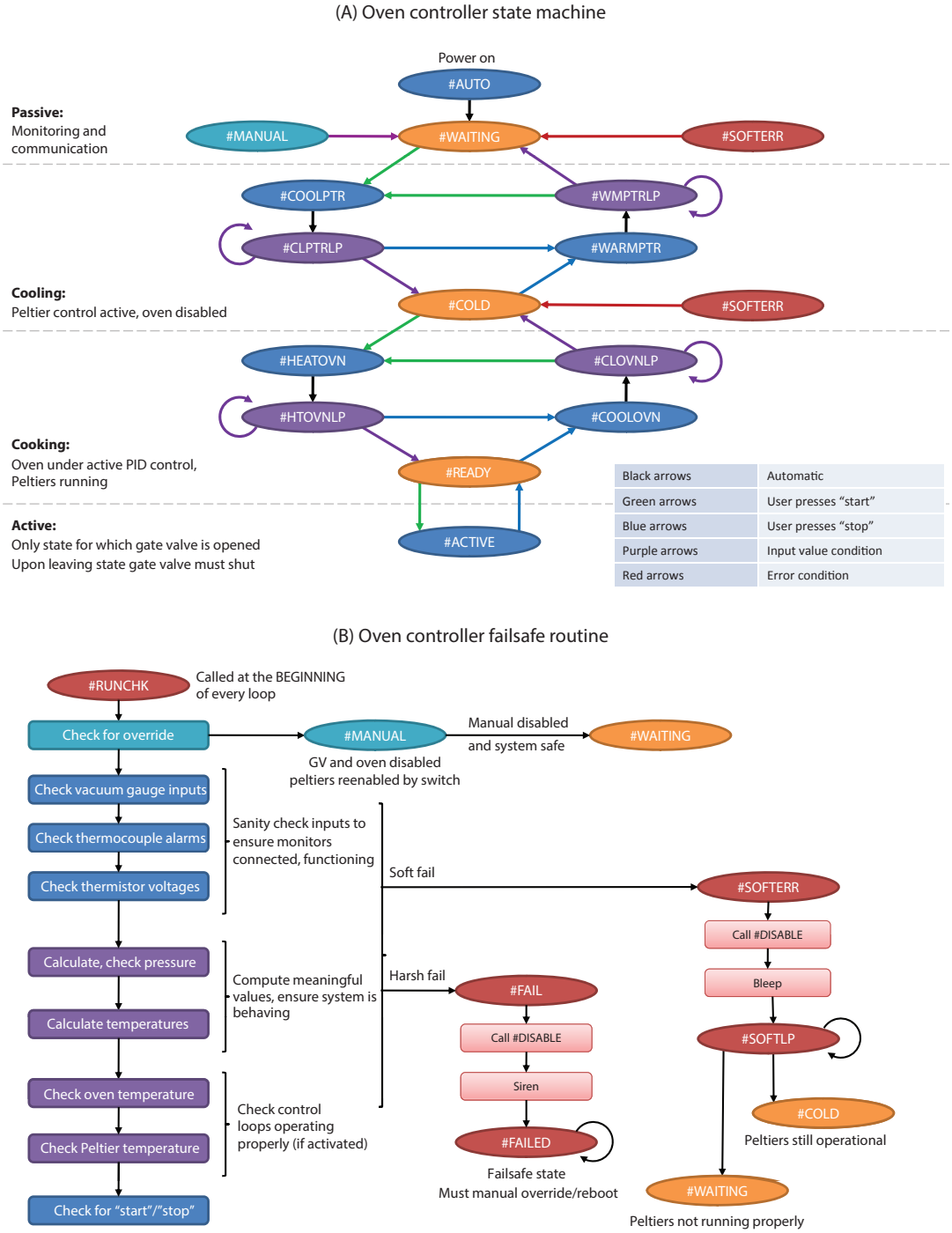

Figure 4.11: *The controller state-machine (A) keeps the apparatus in a well-defined state. A variety of sensors are continually checked (B) to detect an error, entering one of two fail-safe modes depending on severity. User intervention is explicitly required to resume operation from a harsh fail, preventing the oven from entering a potentially dangerous state without diagnosis.*

4.4: BIAS: A modular image acquisition system

The experimental apparatus is operated by a modular set of control system programs developed in-house, called the LABSCRIPT SUITE [157]. The `labscript` language provides a set of extensions to standard `python` that enables experiments to be described in terms of a series of events, abstracting away the low-level implementation details about how devices are programmed or connected. The script is compiled to hardware instructions that are stored in an HDF5 file [158] that encapsulates all data relating to a single realisation of the experiment (a 'shot'). This hierarchical scientific data format enables experimental inputs (script, parameters, settings) to be stored with outputs (acquisitions, images, debug information) for each time the experiment is run, automatically keeping a detailed log of past experimental runs.

The suite is divided into several applications, each performing a different function (Figure 4.12). This modular design enhances separation of high-level experimental logic from low-level device implementation details by allowing modules to operate at different levels of abstraction. The individual components communicate over a network connection, allowing different applications (and different hardware) to be run from different computers and improving real-time diagnostic abilities.

Another advantage of the modularity is that it enables 'secondary' control programs to be used to communicate with specific devices when software to do so exists and has been written and debugged. In particular, this is valuable for software written in another programming language that would take significant time to rewrite and debug as part of the core suite. One such module is the program responsible for controlling camera hardware and providing interactive image capture, the BEC Image Acquisition

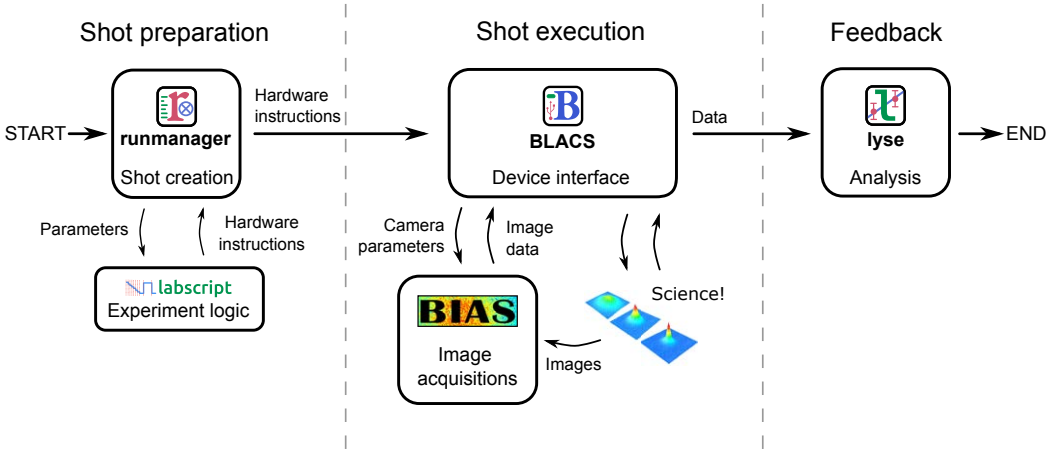

Figure 4.12: *Interaction between modules of the Labscript suite. An experiment is defined in `labscript` logic, which is converted to hardware instructions by `runmanager`. `BLACS` coordinates experiment execution and manages hardware programming, interfacing with secondary programs like `BIAS`. Once a shot is complete it is post-processed and analysed by `lyse`. Adapted from [157].*

System (BIAS).

The primary purpose of BIAS is to take hardware-agnostic instructions (such as exposure time, number of frames to capture, regions of interest) and to program attached cameras in an interchangeable way, translating instructions into commands accepted by the particular software development kit (SDK) in use. BIAS also performs image processing tasks such as background subtraction, saturation correction, optical depth calculation, and simple 2D fitting (Figure 4.13).

As per the rest of the LABSCRIPT SUITE, this is achieved with object orientation [157]. An abstract base class ('Camera') defines an interface to a generic device, and child classes extend this interface with SDK-specific implementation of instructions, and manufacturer-specific special cases where necessary. The net result is that once implemented, swapping between camera types and toolkits is seamless in the experimental script.

BIAS was written in LabVIEW to take advantage of the native image processing and display functionality, and availability of hardware drivers from many different manufacturers. Sequences of images can be captured and displayed, regions of interest highlighted, and calculations such as optical depth or profile fits performed (Figure 4.14). Regions of interest can be selected for capture or fitting, to reduce camera readout time or computation time.

The LABSCRIPT SUITE uses the HDF5 file format to encapsulate all instructions, data and metadata for a single shot in a single hierarchical file. At the time of writing the application, there was no native support for HDF5 in LabVIEW, and only a slow legacy library existed to provide an interface. Having determined that reading and writing large quantities of data was a bottleneck for operation, I created a fast new

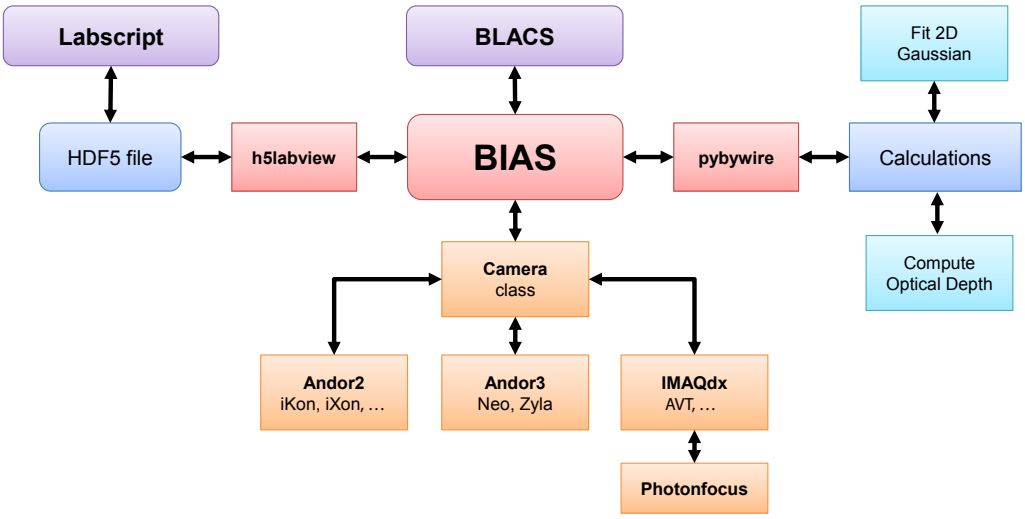

Figure 4.13: *A simple overview of the components of BIAS and how it integrates with the rest of the* LABSCRIPT SUITE *of programs.*

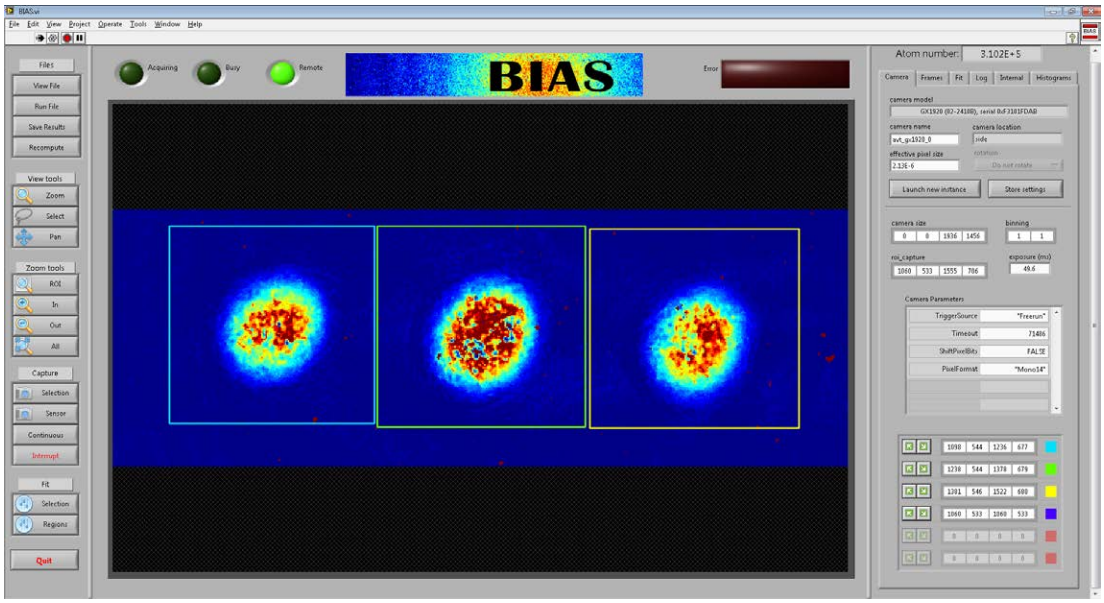

Figure 4.14: *Screenshot of `BIAS` in operation, showing the three spin components of a BEC Stern-Gerlach separated. Multiple regions of interest have been defined to allow each component to be subsequently analysed.*

language bindings to the HDF5 file format. Termed `h5labview` [159], it was released as an open-source package and has been developed to provide a robust and fast interface to storing large hierarchical datasets in `LabVIEW`. It has since acquired a broad user base, and is used for scientific data storage by several groups worldwide.

Performing non-trivial calculations on large datasets (such as 2D curve-fitting) is also cumbersome in `LabVIEW`. The rest of the LABSCRIPT SUITE is written in `python`, which has a rapidly growing code-base of scientific and numerical code. To leverage this potential and enable code-sharing with the `lyse` analysis routines, I wrote the `pybywire` library [160] to enable the execution of arbitrary `python` code from `LabVIEW`. It uses ZeroMQ [161] for reliable data transfer and MessagePack [162] for serialisation, for which I also created `LabVIEW` interfaces [163, 164].

`BIAS` provides an extensible platform for image capture, display and analysis. Its object-oriented interface permits camera interoperability, and its data input/output routines enable it to both integrate with the wider LABSCRIPT SUITE and execute scripts in other languages.

4.5: Summary

In this chapter I described the apparatus we constructed for the creation and study of spinor BECs, with the goal of reliable and autonomous execution of experiments. An overview of the apparatus design was given, with specific details on the aspects of our implementation most relevant to the proposed experiments provided. I described several components of the wider system were described in depth, comprising the parts of the system I developed.

A digital offset-locking technique was developed and implemented to lock the Zeeman repump laser at an arbitrary detuning using a phase-frequency detector to analyse the beatnote with another laser. The single-featured error signal generated this way is robust, and by digitally adjusting the counter settings the lock point can be changed. This enabled the detuning to be optimised to improve the efficiency of the Zeeman slower.

A fail-safe oven controller was designed and constructed using a programmable logic controller to operate the oven and continuously monitor its state, automatically taking action to render the oven safe in the event that a dangerous situation is detected. Water cooling failures have triggered the fail-safe on multiple occasions, and the controller has prevented damage to the apparatus by taking immediate action.

A modular imaging application was developed to capture and process data from a number of different camera types, presenting a unified interface and integrating with the rest of the LABSCRIPT control suite used to operate our apparatus and execute experiments. The techniques and interfaces developed to exchange data with HDF5, ZeroMQ and python were packaged into a number of open-source projects which have developed a wide user base.